Polymer 50 (2009) 5693–5700

Contents lists available at ScienceDirect

Polymer

journal homepage: www.elsevier.com/locate/polymer

Immobilization of carbonic anhydrase by embedding and covalent coupling into nanocomposite hydrogel containing hydrotalcite

Ya-Tao Zhang [a,b], Tian-Tian Zhi [a], Lin Zhang [a,*], He Huang [c], Huan-Lin Chen [a]

[a] College of Chemical and Biochemical Engineering, Zhejiang University, Hangzhou 310027, People's Republic of China
[b] School of Chemical Engineering and Energy, Zhengzhou University, Zhengzhou 450001, People's Republic of China
[c] College of Life Science and Pharmaceutical Engineering, Nanjing University of Technology, Nanjing 21009, People's Republic of China

ARTICLE INFO

Article history:
Received 3 November 2008
Received in revised form
18 September 2009
Accepted 26 September 2009
Available online 13 October 2009

Keywords:
Activated nanocomposite hydrogel
Hydrotalcite
Immobilization of carbonic anhydrase

ABSTRACT

Poly(acrylic acid-co-acrylamide)/hydrotalcite (PAA-AAm/HT) nanocomposite hydrogels activated by *N*-hydroxysuccinimide (NHS) in the presence of *N*, *N*'-dicyclohexylcarbodiimide (DCC) were used to immobilize carbonic anhydrase (CA) by embedding and covalent coupling. Cryo Scanning Electron Microscope (CryoSEM) proved the presence of free water in the porous network structures of the swollen hydrogels. Fluorescence microscopy indicated the existence of the immobilized enzyme in the hydrogels. Compared with un-activated hydrogels, activated hydrogels could improve the amount of the immobilization of enzyme, and maximum enzyme loading is about 4.6 mg/g of support for the activated hydrogels. The porous embedding and multi-point covalent linkage between enzyme and hydrogels strengthened the secondary structure stability of enzyme and thus enhanced enzyme stability in the presence of organic solvent and at high temperature. The immobilized enzyme in the activated hydrogel with enhanced structural stability offers great potential as a method to stabilize enzyme for various applications.

1. Introduction

Carbonic anhydrase (CA) is a zinc metalloenzyme that efficiently catalyzes the reversible hydration of carbon dioxide to bicarbonate and a proton with a maximum turnover rate of 10^6 mol [CO_2] mol^{-1} [CA] sec^{-1}. CA is the most efficient catalyst for CO_2 hydration and dehydration, particularly for application at low pCO_2. Great efforts have been focused on the exploration of CA catalysis in, such as, CO_2 adsorption in a space shuttle or a submarine, CO_2 hydration in an oxygenator, CO_2 reduction in the atmosphere, and the enrichment of natural gas [1–4].

The specificity of enzyme promises great improvements in various applications such as chemical conversions, biosensor, and bioremediation. However, the short catalytic lifetime of enzyme presently limits their usefulness. Immobilization of enzyme has been taken to improve catalytic stability of enzymes and can expand the applications of the natural catalysts [5,6]. There are many materials, including polymers and inorganic supports, to be used to immobilize enzyme, and good activity retention and enhanced thermostability are often observed [7–14].

Many attempts have been made to immobilize CA, and encapsulation of CA can provide an efficient route to enhance enzyme stability. For example, coating CA with a Michael-adduct-based membrane could retain only 7% of the original activity [15]. The uniform CA nanogel with enhanced structural stability against denaturation and aggregation expands the applications of CA catalysis, particularly those carried out at high temperatures. However, enzyme stability in the presence of organic solvent was not investigated [16]. Another source of considerable is hydrogels. Porous superabsorbent hydrogels display advantageous for using in pharmaceutical field, e.g. as scaffold for cell growth because they present adequate sites for attachment and growth of enough cells to survive in vitro [17,18]. Thereby, there has been an increasing interest on the synthesis of hydrogels for enzyme immobilization. Several researchers reported that hydrogel carriers such as poly(acrylamide-co-acrylic acid), and Ca-alginate provide a protective microenvironment for enzymes and yield higher stabilities [19,20]. Simultaneity, in our previous work, poly(acrylic acid-co-acrylamide)/hydrotalcite (PAA-AAm/HT) nanocomposite hydrogels have been used to immobilize CA and could retain over 85% of the enzyme activity [21]. The reason may lie on the formation of a microenvironment almost all composed of free water inside the network porous of the hydrogel. However, free water in the network porous of the hydrogel has not been proved. Furthermore,

* Corresponding author. Tel.: +86 571 87952121; fax: +86 571 87953802.
E-mail address: linzhang@zju.edu.cn (L. Zhang).

0032-3861/$ – see front matter © 2009 Elsevier Ltd. All rights reserved.
doi:10.1016/j.polymer.2009.09.067

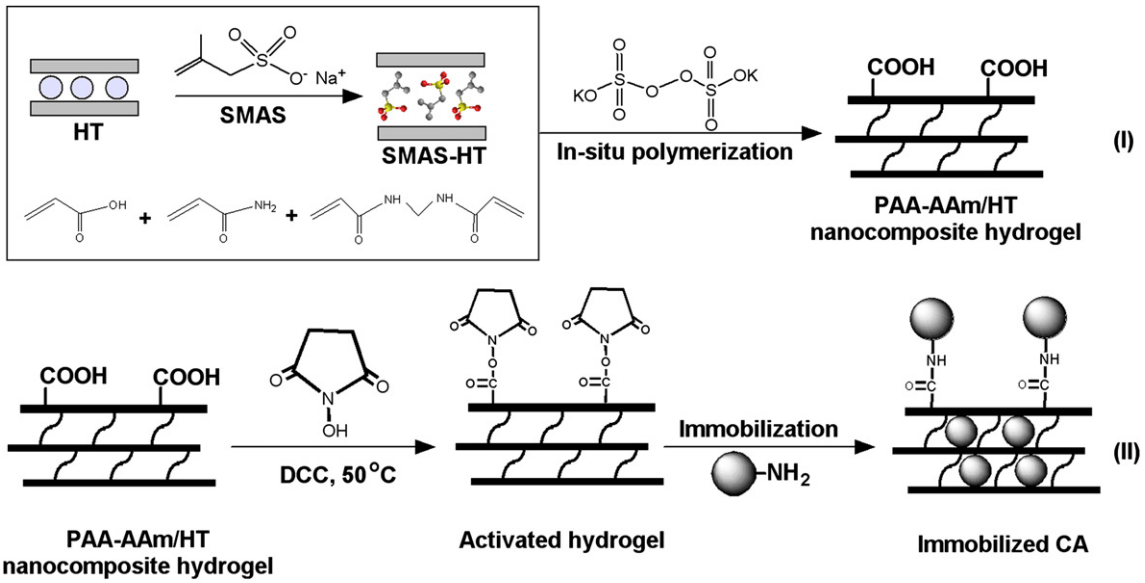

Fig. 1. Procedure for carbonic anhydrase immobilization by activated PAA-AAm/HT nanocomposite hydrogels.

the amount of the immobilization of enzyme is lower. In order to enhance the amount of the immobilization of enzyme, PAA-AAm/HT nanocomposite hydrogels could be activated by *N*-hydroxysuccinimide and then used to immobilize CA enzyme. The porous embedding and multi-point covalent linkage between CA molecules and the hydrogels will improve the amount of the immobilization of enzyme, but also strengthen the secondary structure stability and thus enhanced enzyme stability in the presence of organic solvent or at high temperature. Therefore, the immobilized CA in the activated nanocomposite hydrogel with enhanced structural stability offer great potential as a method to stabilize enzyme for various applications.

Herein, PAA-AAm/HT nanocomposite hydrogels were firstly activated by *N*-hydroxysuccinimide (NHS) in the presence of *N*, *N*'-dicyclohexylcarbodiimide (DCC). And then, activated hydrogels were used to immobilize carbonic anhydrase (CA). The CO_2 hydration activities of free enzymes and immobilized enzymes were evaluated in detail. The amounts of the enzyme immobilized in the hydrogels before and after activation were also compared. The method has shown some interesting and valuable advantages, such as, high amount of the immobilization and improved stability in the presence of organic solvent and at high temperature.

2. Experimental

2.1. Materials

Acrylic acid (AA, C.P.) and acrylamide (AAm, A.R.) were purified by rotary evaporation at 74 °C/25 mmHg and recrystallization in acetone to remove polymerization inhibitor, respectively. *N*, *N*'-methylenebisacrylamide (NMBA, A.R.), kalium persulfate (KPS, A.R.), trishydroxymethylaminomethane (Tris, B.R.), and *N*, *N*'-dicyclohexylcarbodiimide (DCC, C.P.) were bought from Sinopharm Chemical Reagent Co., Ltd, China. Sodium methyl allyl sulfonate (SMAS, 99%) was purchased from Aldrich. *N*-hydroxysuccinimide (NHS) was bought from J&K Chemical Ltd. Bovine carbonic anhydrase type II (CA) was purchased from Worthington Biochemical Corporation. Fluorescein Isothicyanate (FITC) was purchased from Bio Basic Inc. Other chemicals were of analytical grade and used without further purification.

2.2. Preparation of hydrotalcite and intercalated hydrotalcite (SMAS–HT)

Hydrotalcite (HT) was prepared by "urea" method [22]. 0.15 mol $Mg(NO_3)_2 \cdot 6H_2O$, 0.075 mol $\cdot Al(NO_3)_3 \cdot 9H_2O$ and some urea were dissolved in 250 ml distilled water under stirring. The urea/NO_3^- ratio in the solution was controlled as 2. When the temperature was higher than 90 °C, urea began to dissolve and gas evolved from the solution. The pH of the solution began to rise simultaneously. The precipitate began to appear when the pH reached 7 after 1 h, the solution turned into slurry after further 10 min. The slurry was heated at 95 °C for 10 h under stirring, and then was aged statically at the same temperature for another 20 h. Finally, the resulting precipitate was washed several times with distilled water and dried at 90 °C.

Before in-situ polymerization, HT needs to be modified organically. Herein, HT was intercalated by SMAS according to the former report [23]. HT and SMAS were mixed in 500 ml *N*, *N*'-dimethylacetamide. And then, the suspension solution was stirred at 78 °C

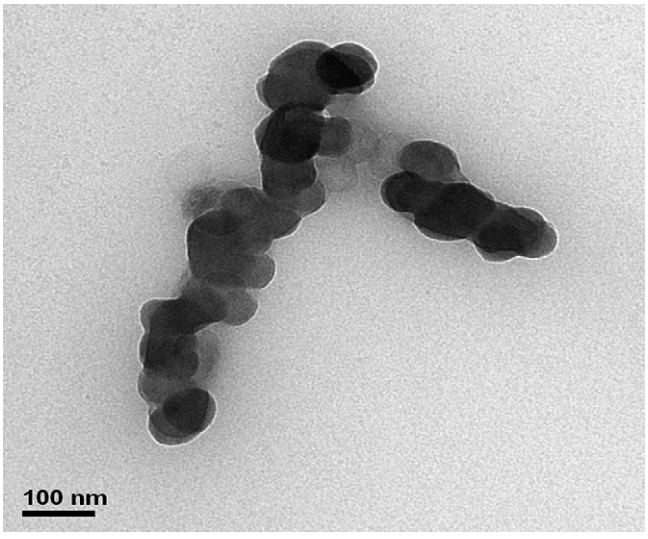

Fig. 2. Granule morphology of dried nanocomposite hydrogel (nanohydrogel-C).

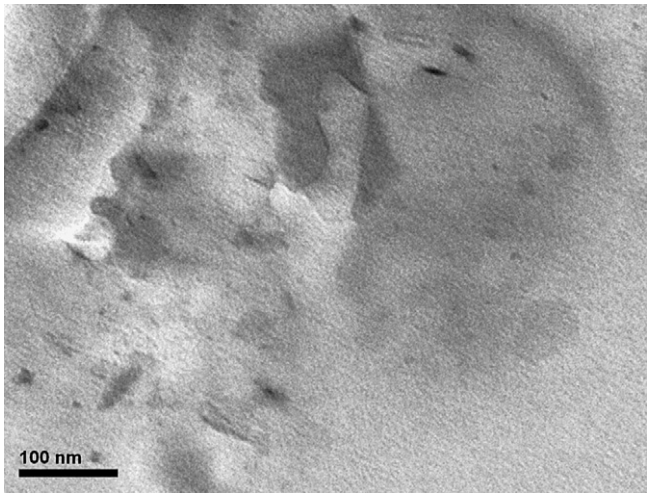

Fig. 3. Microstructure of exfoliated HT nanolayers in the PAA-AAm matrix.

for 24 h in a 1000 ml three-neck flask equipped with a stirring device, a reflux condenser, and a thermometer. The organo-modified HT (SMAS–HT) was filtered and dried in a vacuum drying cabinet at 70 °C for 24 h.

2.3 Preparation of PAA-AAm/HT nanocomposite hydrogels

According to our previous work [21], the preparation of PAA-AAm/HT nanocomposite hydrogels was carried out as follows. Firstly, 22.5 g AA neutralized by NaOH solution, 2.25 g AAm, 0.0045 g NMBA, 0.045 g KPS, 150 ml cyclohexane, 0.99 g Span 60, and the appropriate amount of SMAS–HT (1 wt%, 2 wt%, 3 wt%, 4 wt%, and 5 wt%) were added into the a 500 ml four-neck kettle equipped with a reflux condenser header, a stirring rod (PTFE, 300 × 70 mm and 500 r/min), and a thermometer. And then, air was flushed from the kettle by introducing N_2 until the reaction was over. The polymerization was divided into two stages, 50 °C for 1 h and 60 °C for 2 h. Finally, the product was filtered, washed, and dried in a vacuum drying cabinet at 70 °C for 24 h. The samples were marked with nanohydrogel-A (1 wt% SMAS–HT), nanohydrogel-B (2 wt% SMAS–HT), nanohydrogel-C (3 wt% SMAS–HT), nanohydrogel-D (4 wt% SMAS–HT), and nanohydrogel-E (5 wt% SMAS–HT). The preparation procedure for PAA-AAm/HT nanocomposite hydrogels is shown in Fig. 1 (I).

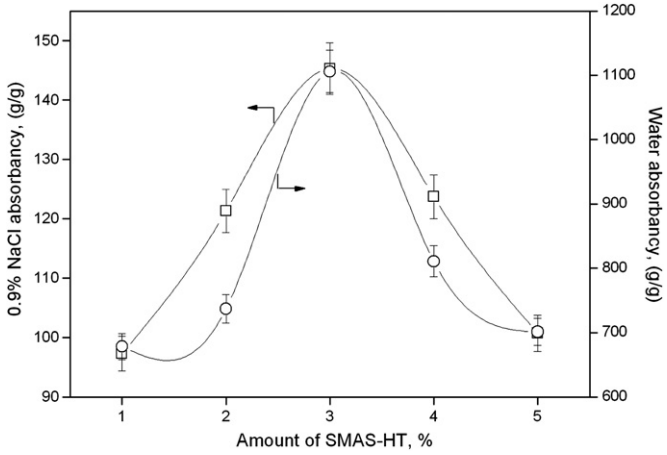

Fig. 4. Effect of SMAS–HT content on absorbency in de-ionized water and 0.9 wt% $NaCl_{(aq)}$.

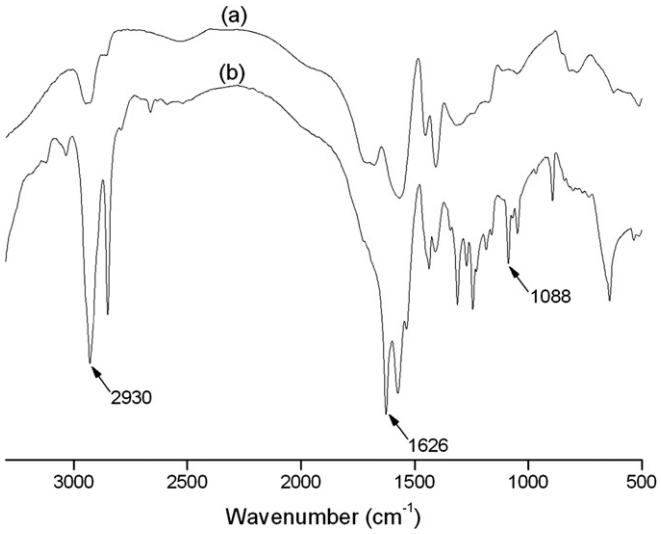

Fig. 5. FTIR spectra of un-activated hydrogel (a) and activated hydrogel (b).

2.4. Activation of PAA-AAm/HT nanocomposite hydrogels by NHS

0.2 g PAA-AAm/HT nanocomposite hydrogel, 0.8 g NHS, and 1.4 g DDC were dispersed in the 200 ml ethanol. The reaction was carried out with stirring at 50 °C for 24 h. The products were filtered, washed, and dried in a vacuum drying cabinet at 70 °C for 24 h. The samples were marked with activated nanohydrogel-A (1 wt% SMAS–HT), activated nanohydrogel-B (2 wt% SMAS–HT), activated nanohydrogel-C (3 wt% SMAS–HT), activated nanohydrogel-D (4 wt% SMAS–HT), and activated nanohydrogel-E (5 wt% SMAS–HT).

2.5. Immobilization of CA enzyme

Firstly, 0.1 g activated hydrogels were introduced into Tris–HCl buffer solution (20 ml, pH 8.0). And then, enzyme solution (5 ml, 0.1 g/l) prepared with Tris–HCl buffer solution were added into the swollen hydrogels. The immobilization reaction of enzyme was carried out in the table concentrator at 4 °C for 4 h. Finally, the hydrogels with immobilized enzyme were completely washed by Tris–HCl buffer solution until the absorbance of wash filtrate at 280 nm was unchangeable. The procedure for enzyme immobilization with the activated hydrogels is shown in Fig. 1 (II).

2.6. Fourier transform infrared spectroscopy (FTIR)

FTIR was recorded from pressed KBr pellets containing about 1% of the hydrogel and activated hydrogel, respectively, using a Nexus-670 (Nicolet, USA).

2.7. Cryo scanning electron microscope (CryoSEM)

Porous microstructures of hydrogels were examined by Cryo Scanning electron microscope (CryoSEM) (S-3000 N, Hitachi, Japan) including refrigerating equipment (Alto-2100, Gatan, U.K.). Swollen hydrogels were frozen at −160 °C, and then sublimated at −95 °C for 5 min, finally, gold sputter-coated before observation by CryoSEM analysis. In those conditions it can be assumed that the porous microstructures of the swollen hydrogels were preserved. In addition, to prove the present of free water in the porous structures of hydrogels, the swollen hydrogels were frozen at −160 °C but did not sublimate.

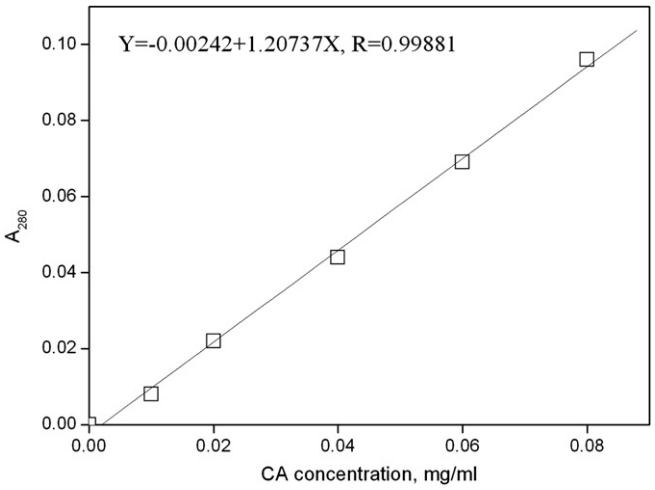

Fig. 6. Standard calibration curve of UV absorption at 280 nm to concentration of CA.

2.8. Transmission electron microscopy (TEM)

The dispersion of exfoliated HT sheets in the matrix was obtained by TEM (JEM-1230, JEOL, and Japan) at an acceleration voltage of 100 kV. Ultrathin films for TEM were prepared by cutting from the epoxy block with the embedded dried swollen hydrogels at room temperature using an ultramicrotome (ULTRACUT E, Reichert-Jung, Austria). Moreover, morphology of hydrogels was examined by TEM. Samples were dispersed in ethanol solvent with supersonic vibration 30 min. Then drops of the solution were placed on the copper TEM grid, and dried at room temperature.

2.9. Fluorescence microscopy

In order to observe the presence of enzyme immobilized in the hydrogels, the fluorescence microscopy (Olympus BX-51) was used. CA enzyme was firstly labeled by FITC reagent and dialyzed for 24 h. Then, labeled enzyme was added into the swollen hydrogel and shaken in the table concentrator for 12 h. Finally, the hydrogel with immobilized enzyme was frozen at liquid nitrogen and then was sliced.

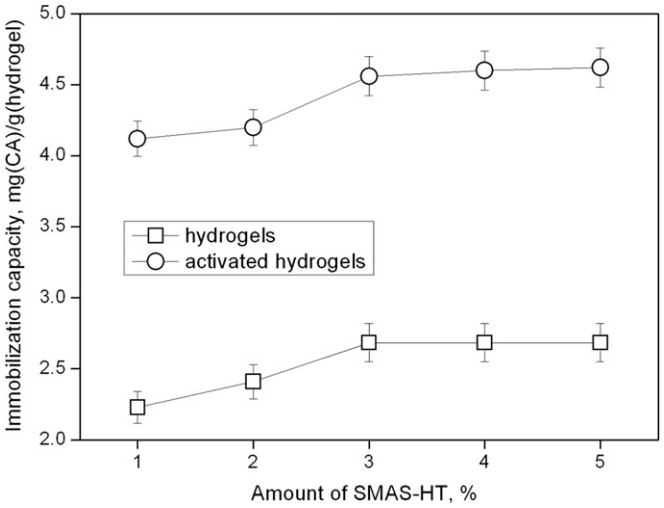

Fig. 7. Comparison of immobilization capacity of un-activated hydrogels and activated hydrogels.

2.10. Water (salt) absorbency of hydrogels

Water absorbency was measured by the tea-bag method [24,25]. A 100-mesh nylon bag containing 0.3 g sample was immersed in 500 ml de-ionized water or 200 ml 0.9 wt% NaCl $_{(aq)}$ for 2 h to reach swelling equilibrium. And then, the swollen hydrogel was hung up for 30 min. The equilibrium absorbency Q was calculated by use of the following equation, in which m_1 and m_2 are the weights of the dry sample and the swollen sample, respectively.

$$Q = \frac{m_2 - m_1}{m_1}$$

2.11. Hydrase activity assay

Hydrase activity was determined by the calorimetric method [26]. 0.2 ml enzyme solution and 8 ml saturated CO_2 solution at 2 °C were added into 12 ml Tris–HCl buffer solution, pH 8.3 at 2 °C. The time required for the pH to change from 8.3 to 6.3 was recorded by a pH meter (pH 1100 series, Oakton). The hydrase activity was determined according to the following equation, in which T_0 and T represent the time required for the pH to change from 8.3 to 6.3 in the reaction without and with enzyme, respectively.

$$U = 20(T_0/T - 1)/(\text{mg protein})$$

For the immobilized enzyme, a certain amount of hydrogels with immobilized CA were added into the buffer solution and maintained constant temperature in the mixed ice water bath. And then, the saturated CO_2 solution was added and the time required for the pH to change from 8.3 to 6.3 was recorded. Finally, the hydrase activity was determined according to the same equation.

2.12. Immobilization capacities of hydrogels and activated hydrogels

The swollen hydrogels with immobilized enzyme were completely washed by buffer solution until the absorbance of wash filtrate at 280 nm was unchangeable. The absorbance at 280 nm was tested by UV-VIS spectrophotometer (LengGuang Tech., Spectrumlab-54) with the blank solution as the control. The amounts of enzyme before and after immobilization were determined by the calibration curve. Therefore, the immobilization capacities were gotten according to the difference of enzyme before and after immobilization.

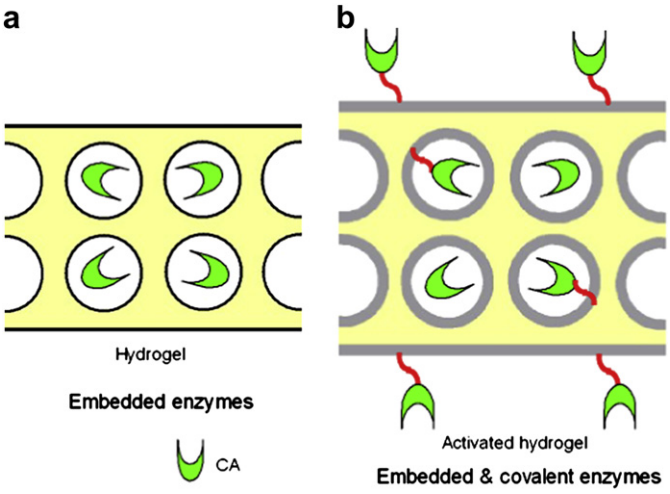

Fig. 8. Schematic diagram of embedded enzymes for un-activated hydrogels (a) and embedded and covalent enzymes for activated hydrogels (b).

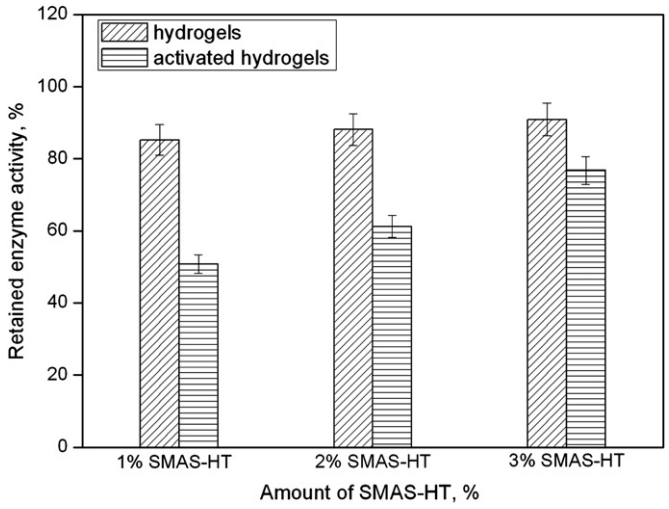

Fig. 9. Enzymatic activity of immobilized enzymes by un-activated hydrogels and activated hydrogels.

2.13. Thermal stability and resistance to organic solvent of free CA and immobilized CA

The free and immobilized enzymes were placed in the buffer solution (pH = 8.0) at 50 °C. In one hour, activities of free and immobilized enzyme were tested at various time intervals. Similarly, the free and immobilized enzymes were added into methanol, ethanol, and acetone, respectively. Activities of free and immobilized enzyme were tested after incubated for 0.5 and 1 h in the organic solvents, respectively.

3. Results and discussions

3.1. Morphology and water (salt) absorbency of PAA-AAm/HT nanocomposite hydrogel

Morphology of dried nanocomposite hydrogel is shown in Fig. 2. PAA-AAm/HT nanocomposite hydrogels obtained by inverse suspension polymerization disperse uniformly in the form of regular spherical particles and sizes are around 100 nm. In addition, TEM technique confirmed the exfoliated structure of PAA-AAm/HT nanocomposite hydrogel. The microstructure of the nanocomposite hydrogels is clearly accompanied by the TEM pattern (see Fig. 3). Exfoliated layers of HT were prevalent, and some primary particles, with their thickness less than 60 nm, were also observed. Consequently, after appropriate organo-modification by SMAS, HT was exfoliated and dispersed in PAA-AAm matrix on a nanoscale to form a new polymeric nanocomposite hydrogel. The nanolayers of HT were exfoliated and well dispersed in the polymer matrix, causing more $[Mg_{1-x}Al_x\cdot(OH)_2]$ nanolayers formation and providing a stronger hydration ability of the hydroxyl group [23]. Therefore, PAA-AAm/HT nanocomposite hydrogels became more hydrophilic. In our previous work, the morphology of hydrogels and exfoliated structure of HT in the hydrogels have been gotten [21].

The water (salt) absorbency in de-ionized water and 0.9 wt% $NaCl_{(aq)}$ measured by the tea-bag method are shown in Fig. 4. The results showed that the water (salt) absorbency of the hydrogels increased with increasing content of SMAS–HT. It was because that between the vinyl groups of SMAS and the vinyl groups of acrylic acid generates the crosslink, imparting greater compatibility of the nanocomposite hydrogels. Moreover, HT could act as an additional network point. The cross-linking density of the hydrogels increased with increasing content of SMAS–HT [24,25]. And then, the SMAS–HT became the cross-linking point of the absorbent network and the chains of the effective absorbent network became longer. Therefore, the water (salt) absorbency increased with increasing appropriate content of SMAS–HT. According to Flory's swelling theory [27], water/salt absorbency achieved the maximum with increasing the cross-linking degree. The highest absorbency of the hydrogels for 0.9 wt% $NaCl_{(aq)}$ could be up to 145 g/g. However, water absorbency would decrease if the cross-linking degree was excessively great. This was because that the excessive cross-linking degree would result in smaller pore size of the porous structure.

3.2. Immobilization capacities of hydrogels and activated hydrogels

If the nanocomposite hydrogels were used to immobilize enzyme by only embedding or adsorption, the immobilization capacity of hydrogels was lower and the immobilized enzymes could be leaked easily from the hydrogels. Therefore, in order to improve the immobilization capacity of nanocomposite hydrogels, the hydrogels are activated by NHS in the presence of DCC. Fig. 5 shows the FTIR of the hydrogels and activated hydrogels. The absorption peaks of $-CH_2$ stretching, C=O stretching and C–N stretching appeared at 2930 cm^{-1}, 1626 cm^{-1} and 1088 cm^{-1}, respectively. The FTIR results proved that the hydrogel was activated by NHS successfully.

In order to get the amount of the immobilization of enzyme, a standard calibration curve of CA concentration to UV absorbance at 280 nm was obtained by varying the concentrations of CA in the buffer solution. Fig. 6 reflects that the correlation coefficient is as high as 0.99881 (the value of $\sqrt{R^2}$), indicating a very good linear relationship achieved in the experiment. The immobilization capacity of hydrogels and activated hydrogels is shown in Fig. 7. The results showed that the immobilization capacity of the hydrogels and activated hydrogels increased with increasing content of

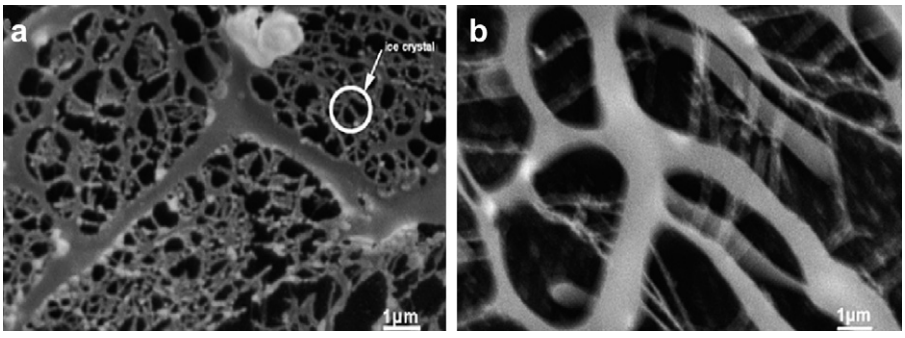

Fig. 10. Porous structures of swollen hydrogels containing free water (a) and without free water (b).

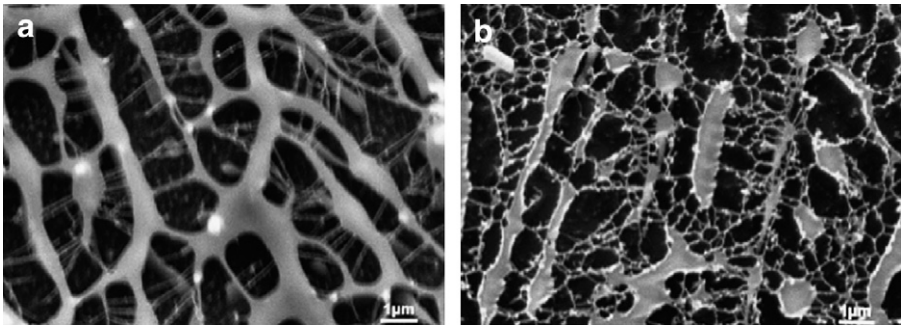

Fig. 11. Microstructure of activated hydrogels before (a) and after enzyme immobilization (b).

SMAS–HT. This was because that the water (salt) absorbency of the hydrogels increases with increasing content of SMAS–HT and the reason had been interpreted in the 3.1 section. Importantly, compared with the hydrogels and activated hydrogels, the immobilization capacity of the activated hydrogels was more than twice as large as that of the hydrogels. Maximum enzyme loading is about 4.6 mg/g of support for the activated hydrogels. It was mainly because that the activated hydrogels were used to immobilize enzyme by embedding and multi-point covalent linkage between amino groups of CA molecules and the activated hydrogels. However, un-activated hydrogels were used to immobilize enzyme by merely embedding or adsorption. In order to better illustrate the results, Fig. 8 shows the schematic diagram of embedded enzymes (a) for un-activated hydrogels, and embedded and covalent enzymes (b) for activated hydrogels.

3.3. Hydrase activity of free CA and immobilized CA

From Fig. 9, nanohydrogel-A, nanohydrogel-B, and nanohydrogel-C could retain 85.2%, 88.1%, and 90.9% of the specific activity of the free enzyme, respectively. Whereas, activated nanohydrogel-A, activated nanohydrogel-B, and activated nanohydrogel-C retained 50.8%, 61.2%, and 76.8% of the specific activity of the free enzyme, respectively. Obviously, the activities of immobilized enzymes for the hydrogels and activated hydrogels increased with increasing content of SMAS–HT. This was attributed that the water absorbency of the hydrogels increased with increasing content of SMAS–HT (see 3.1 section). More and more free water inside the porous structure of the hydrogels could provide a nicer survival condition for the enzymes. In addition, compared with un-activated hydrogels, activated hydrogels could retain lower enzyme activities. It was because that multi-point covalent linkage would partially destroy the active sites of CA. In despite of this, activated hydrogels still retained over 50% of the specific activity of the free enzyme.

A significant reduction in apparent enzyme activity was often observed in enzyme immobilization [15,28]. The reduction in enzyme activity was mainly due to the rigid matrix as an envelope that hindered the access to the enzyme by its substrate, that is, the mass transport resistance or the steric hindrance [2]. In comparison, porous hydrogels or activated hydrogels had only a minor effect on the apparent activity of the enzyme. This was the major advantage of hydrogels that a microenvironment was formed composed of free water in the porous structure of the hydrogels. Free water could provide a nicer survival condition for the enzymes. And that, more hydrophilic hydrogels had also effectively inhibited the aggregation driven by intermolecular hydrophobic and porous hydrogels strengthened the molecular structure of CA, that is, hydrophilic polymers could prevent the protein aggregation [29,30].

To demonstrate the free water in the porous structures of hydrogels, the microstructure of the swollen hydrogels were observed by CryoSEM. Fig. 10(a) is the microstructure of swollen hydrogels which are only frozen at −160 °C without sublimation, that is, free water is contained in the porous structure of the hydrogels. Fig. 10(b) is the porous structure of swollen hydrogels which are firstly frozen at −160 °C, and then sublimated at −95 °C. In those conditions it could be assumed that the microstructures of the swollen hydrogels were preserved. Some ice crystals in the porous structure are observed obviously in Fig. 10(a). Therefore, free water in the porous structures of hydrogels was proved successfully.

In order to study the microstructure change of activated hydrogels before and after enzyme immobilization, the morphology of swollen hydrogels before and after immobilization was observed by CryoSEM (see Fig. 11). It could be seen that the microstructure of activated hydrogels changed a little after

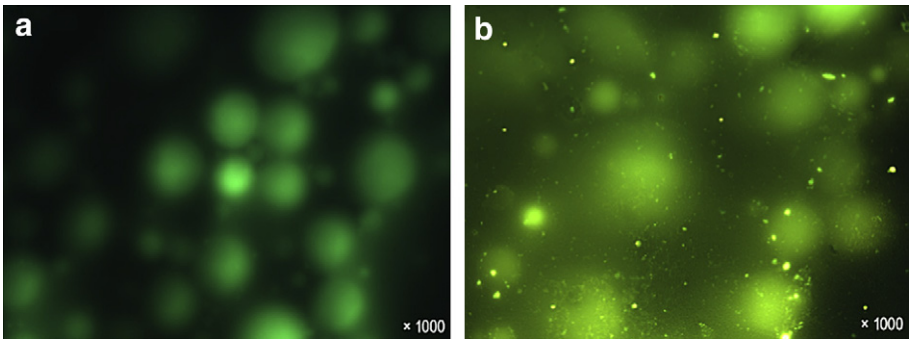

Fig. 12. Fluorescence photos of activated hydrogel (a) and activated hydrogel with immobilized enzyme (b).

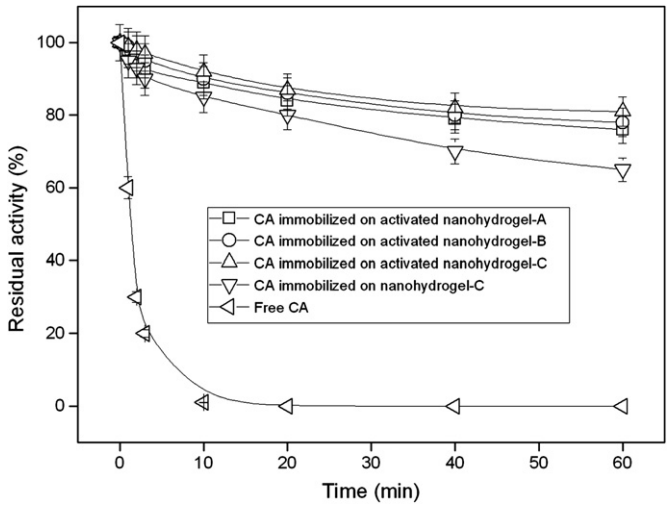

Fig. 13. Thermal stability of free and immobilized enzymes during 60 min incubation period at 50 °C.

immobilizing enzymes and still kept the porous structure. It was observed that they both displayed porous structures due to the formation of gaps. When the hydrogels were immerged in an aqueous media, the CA molecules easily diffused into the network through these gaps [31]. Moreover, in order to determine whether enzymes were successfully immobilized in the activated hydrogels, the fluorescence microscopy was also used. The fluorescence photos of activated hydrogel and activated hydrogel with immobilized enzyme are shown in Fig. 12. Compared with the two fluorescence photos, there were many bright dots in Fig. 12(b). And the bright dots were the fluorescence labeled CA and the results could prove that CA was successfully immobilized among the activated hydrogels.

3.4. Thermal stability and resistance to organic solvent of immobilized enzymes

The thermal stability of the enzyme is one of the most important factors for its application. Thermal stability experiments were carried out with free and immobilized enzymes by activated hydrogels, which were incubated in the Tris–HCl buffer solution at 50 °C and the enzyme activity was measured at various time intervals and following the procedure described earlier (see Fig. 13). Covalently immobilized enzyme showed better thermal stability at all time periods. At 50 °C, free CA lost almost all of its activity during 60 min incubation period, while covalently immobilized enzymes retained their activities at levels of about 80%. In our previous study, the embedded enzymes in the un-activated hydrogels retained their activities at levels of about 65% during 60 min incubation period at 50 °C [21]. The resistance to organic solvent of free and immobilized enzymes by activated hydrogels was also investigated in methanol, ethanol, and acetone. Enzyme activity was tested after incubated for 0.5 and 1 h in the organic solvents, respectively. From Fig. 14, it could be seen that covalently immobilized enzyme showed better resistance to organic solvents than that of free enzyme.

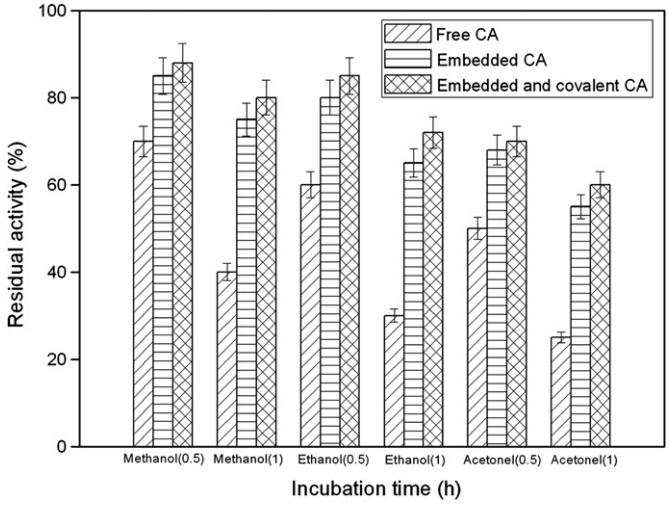

Fig. 14. Resistance to organic solvent of free and immobilized enzymes in methanol, ethanol and acetone.

These results demonstrated that the thermal stability and organic solvent resisting of covalently immobilized CA were better than that of free and embedded CA since the formation of a covalent bond between the enzyme and activated hydrogels prevented the conformation transition of the enzyme and three dimensional structure of enzyme did not affect from immobilization procedure [19,32]. Moreover, covalently immobilized enzymes were performed by multipoint covalent attachment and hence stabilization of immobilized enzyme molecules could be promoted by a microenvironment containing large amount of free water in the porous network structure of these activated hydrogels.

4. Conclusions

Embedded and covalently immobilized enzymes by using activated PAA-AAm/HT nanocomposite hydrogels were investigated in this study. Among the advantages of this approach are: (i) easy immobilization procedure, (ii) high immobilization capacity; (iii) good thermal stability for various biotechnological applications such as a part of enzyme reactor. Experimental results show that three dimensional structure of enzyme did not affect from immobilization procedure. Thermal stability and organic solvent resisting of covalently immobilized CA were showed better than that of free and embedded form. Therefore, it is hopeful to fabricate the hollow fiber membrane bioreactor contained CA immobilized on the activated hydrogels to remove carbon dioxide from air or flue gas.

Acknowledgement

This work was supported financially by the National Natural Science Foundation of China (No. 20776123) and the National Basic Research Program of China (No. 2007CB707805). The authors thank Hanmin Chen (Equipment & Technology Service Platform, College of Life Sciences, Zhejiang University) for CryoSEM analyses.

References

[1] Cowan RM, Ge JJ, Qin YJ, McGregor ML, Trachtenberg MC. Ann N Y Acad Sci 2005;984:453–69.
[2] Yan M, Liu ZX, Lu D, Liu Z. Biomacromolecules 2007;8:560–5.
[3] Zhang YT, Fan LH, Zhang L, Chen HL. Front Chem Eng China 2007;1(3):310–6.
[4] Bond GM, Stringer J, Brandvold DK, Simsek FA, Medina MG, Egeland G. Energy Fuels 2001;15:309–16.
[5] Kim J, Grate JW. Nano Lett 2003;3(9):1219–22.
[6] Wang Y, Hsieh YL. J Memb Sci 2008;309:73–81.
[7] Wang Y, Teng XW, Wang JS, Yang H. Nano Lett 2003;3(6):789–93.
[8] Li S. Biosystems 2004;77(1-3):25–32.
[9] Sheldon RA. Adv Synth Catal 2007;349:1289–307.
[10] Vial S, Prevot V, Leroux F, Forano C. Micropor Mesopor Mat 2008;107:190–201.
[11] Xu S, Peng B, Han X. Eur Polym J 2006;42:2801–2806.
[12] Chang MY, Juang RS. Biochem Eng J 2007;35:93–8.
[13] Ye P, Xu ZK, Wu J, Innocent C, Seta P. Biomaterials 2006;27:4169–76.

[14] Chen JP, Chiu SH. Enzyme Microb Technol 2000;26:359–67.
[15] Drevon GF, Urbanke C, Russell AJ. Biomacromolecules 2003;4:675–82.
[16] Yan M, Ge J, Liu Z, Ouyang PK. J Am Chem Soc 2006;128:11008–9.
[17] Drury JL, Mooney DJ. Biomaterials 2003;24:4337–51.
[18] Schneider GB, English A, Abraham M, Zaharias R, Stanford C, Keller J. Biomaterials 2004;25:3023–8.
[19] Yahşi A, Şahin F, Demirel G, Tümtürk H. Int J Biol Macromol 2005;36:253–8.
[20] Şahin F, Demirel G, Tümtürk H. Int J Biol Macromol 2005;37:148–53.
[21] Zhang YT, Fan LH, Zhi TT, Zhang L, Huang H, Chen HL. J Polym Sci Part A Polym Chem 2009;47:3232–40.
[22] Yang PP, Yu JF, Wang ZL, Liu QS, Wu TH. React Kinet Catal Lett 2004;83:275–82.
[23] Lee WF, Chen YC. J Appl Polym Sci 2004;94:2417–24.
[24] Zhang YT, Fan LH, Cheng LH, Zhang L, Chen HL. Polym Eng Sci 2009;49:264–71.
[25] Zhang YT, Fan LH, Zhao PZ, Zhang L, Chen HL. Compos Interfaces 2008;15(7–9):747–57.
[26] Wilbur KM, Anderson NG. J Biol Chem 1948;176:147–54.
[27] Flory PJ. Principles of polymer chemistry. Ithaca, New York: Cornell University Press; 1953.
[28] Badjic JD, Kostic NM. Chem Mater 1999;11:3671–9.
[29] Lu DN, Liu ZX, Zhang ML, Wang XG, Liu Z. Biochem Eng J 2006;27:336–43.
[30] Lu DN, Liu Z. J Chem Phys 2005;123:141–9.
[31] Guilherme MR, Campese GM, Radovanovic E, Rubira AF, Feitosa JPA, Muniz EC. Polymer 2005;46:7867–73.
[32] Phadtare S, Vinod VP, Wadgaonkar PP, Rao M, Sastry M. Langmuir 2004;20:3717–23.